Available online at www.sciencedirect.com
SCIENCE DIRECT
ACADEMIC PRESS
Journal of Catalysis 218 (2003) 163–177
JOURNAL OF CATALYSIS
www.elsevier.com/locate/jcat

Reactivity of binuclear Fe complexes in over-exchanged Fe/ZSM5, studied by in situ XAFS spectroscopy
2. Selective catalytic reduction of NO with isobutane

A.A. Battiston, J.H. Bitter, and D.C. Koningsberger *

Department of Inorganic Chemistry and Catalysis, Debye Institute, Utrecht University, Sorbonnelaan 16, 3584 CA Utrecht, The Netherlands

Received 11 November 2002; revised 27 February 2003; accepted 3 March 2003

Abstract

In situ XAFS spectroscopy was applied in order to determine the catalytically active sites in Fe/ZSM5, prepared by $FeCl_3$ sublimation. The number of (inactive) spectators in this catalyst was minimized by using a specially dedicated calcination procedure. The catalytic activity of Fe/ZSM5 during the collection of the XAFS data was monitored via chemiluminescence analysis of the gas outlet. Binuclear Fe complexes with a Fe–O–Fe core were found to be catalytically active species in this material. During heat treatment in He to 350 °C the Fe complexes undergo auto-reduction, ascribed to the removal of oxygen from Fe–O–Fe bridges (closest Fe–O-coordination sphere) and the formation of Fe–□–Fe vacancies. Treatment with isobutane results in a further slight average reduction of iron, accompanied by an additional removal of oxygen from the Fe–O–Fe bridges. Fe in the binuclear complexes is readily oxidized when NO, $NO + O_2$, or a typical HC-SCR mixture (NO, i-C_4H_{10}, O_2) is fed to the Fe/ZSM5 catalyst. Reoxidation is accompanied by filling of the Fe–□–Fe vacancies. Under HC-SCR working conditions the average oxidation state of iron is 3+.

Keywords: Fe/ZSM5; Binuclear; Fe; Reactivity; He; O_2; NO; Isobutane; deNO_x; HC-SCR; XAFS; In situ

1. Introduction

Over-exchanged Fe/ZSM5, obtained by chemical vapor deposition (CVD) of $FeCl_3$, has shown a remarkable activity for the decomposition of N_2O [1] and for the selective catalytic reduction of nitrogen oxides using hydrocarbons (HC-SCR), even in the presence of water [2–5]. Catalytic tests have demonstrated that the HC-SCR catalytic activity of Fe/ZSM5 depends on the concentration of oxygen and on the type of hydrocarbon employed in the feed. The highest N_2 yields have been obtained in the 2–10 vol% O_2 range by using n-butane or isobutane as reductant [3].

In order to unravel the HC-SCR reaction pathway on Fe/ZSM5, several studies have been performed by applying in situ FTIR spectroscopy [3,4,6]. Intermediate adsorption species have been monitored while feeding (separately, or at the same time) typical HC-SCR reagents, i.e., NO, O_2, and i-C_4H_{10} (or alternatively, a different alkane). Based on these results, and on catalytic tests performed with labeled reactants, a model for the HC-SCR reaction pathway has been proposed. According to this model, the first HC-SCR steps are believed to be the oxidation of NO by O_2 to form NO_2, which is then released to the gas phase, and the formation and adsorption of nitro $(NO_2)^-$ and nitrate $(NO_3)^-$ complexes. These $(NO_y)^-$ complexes react further with the hydrocarbon, forming organic nitro and nitroso compounds. The nitro/nitroso deposits may evolve through different pathways, depending on the nature of the hydrocarbon. Independent of the type of hydrocarbon employed, the final step in the pathway is proposed to be the reaction of the organic compound with NO_2 from the gas phase, leading to the formation of a N–N bond and the desorption of N_2.

The active species responsible for the peculiar catalytic properties of over-exchanged Fe/ZSM5 are believed to consist of extraframework binuclear Fe-oxo/hydroxo complexes, with a $[OH–Fe–O–Fe–OH]^{2+}$ core [1–3,7,8], ligated to the Brønsted aluminum sites of the zeolite. Several spectroscopic studies have indeed demonstrated that binuclear Fe-oxo/hydroxo complexes are generated by the reaction

* Corresponding author.
E-mail address: d.c.koningsberger@chem.uu.nl (D.C. Koningsberger).

0021-9517/03/$ – see front matter
doi:10.1016/S0021-9517(03)00120-9

of sublimated $FeCl_3$ with the Brønsted protons of the zeolite and by the subsequent hydrolysis processes occurring during washing [9–12]. The Fe-binuclear species in washed Fe/ZSM5 consist of two octahedrally coordinated Fe^{III} oxo/hydroxo ions, with a structure similar that of the closest Fe-binuclear building unit in α-goethite [10,11].

The final treatment in the synthesis of Fe/ZSM5 is calcination. Calcination, applied to stabilize and activate the Fe phase, is a delicate step for the further evolution of the Fe-binuclear complexes. Our group has shown that, if the calcination procedure is not carefully controlled, this treatment can result in the removal of a significant fraction of iron from the zeolite micropores, finally resulting in the formation of large catalytically inactive [8] goethite/hematite crystals [11,13]. On the contrary, by adequately tuning the conditions applied during calcination a high concentration of Fe-binuclear species in Fe/ZSM5 can be preserved. From our EXAFS study [11] binuclear Fe clusters in "mildly calcined" Fe/ZSM5 (Si/Al = 17) are estimated to account for at least 70% of the total iron amount. This material is therefore the best suited for characterizing structure and reactivity of the Fe-binuclear complexes, minimizing the interference of (inactive) spectators.

In a previous paper [14] we have studied the structure of the Fe-binuclear complexes in Fe/ZSM5, measured at 30 °C in He, upon exposure to air. Furthermore, we have focused our attention on the changes occurring in the Fe–O coordination of the iron complexes during heating treatments in He and in a He/O_2 (50/50) mixture. The results obtained, discussed in Ref. [14], are summarized in the model presented in Fig. 1. Upon exposure to air, six Fe–O neighbors have been identified in the as-synthesized Fe/ZSM5. In the model proposed the oxygen atoms have been lumped together in three different Fe–O shells. The closest Fe–O shell (Fe–O_1, 1.85–1.89 Å) has been assigned to a terminal hydroxyl group and to an oxygen atom bridging the Fe ions, according to the $[HO–Fe–O–Fe–OH]^{2+}$ core model proposed by Chen and Sachtler [2]. The Fe–O shell at intermediate distance (Fe–O_2, 1.97–1.99 Å) has been assigned to two oxygen atoms ligating the Fe atoms to the aluminum-centered tetrahedra of the zeolite [14]. The most distant shell

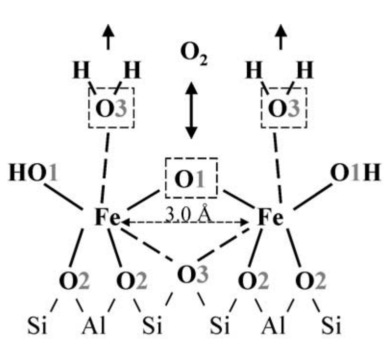

Fig. 1. Proposed structure and reactivity of the binuclear oxo/hydroxo Fe complexes in Fe/ZSM5, obtained by $FeCl_3$ CVD, during heating treatments to 350 °C in helium and in the presence of oxygen [14].

(Fe–O_3, 2.02–2.09 Å) has been attributed to an oxygen atom of the zeolite and to an adsorbed water molecule, respectively.

The assignment of the different Fe–O shells is based on the results obtained during the heat treatments. Heating Fe/ZSM5 to a moderate temperature (up to ∼ 150 °C), in He as well as in the presence of O_2, results in the removal of approximately one oxygen atom (O_3) from the most distant Fe–O shell. Since this is not accompanied by changes in the oxidation state of iron, the oxygen removal is consistent with desorption of weakly bound H_2O. The further evolution of the Fe complexes at higher temperature ($\Delta T = 150$–350 °C) is strongly influenced by the composition of the gas phase. In He a significant fraction of iron undergoes auto-reduction, a phenomenon already known in the literature for over-exchanged Fe/ZSM5 [9,13,15]. This phenomenon coincides with the removal of only one oxygen atom (O_1) from the closest Fe–O shell. The most plausible interpretation appears to be the removal of the Fe–O–Fe bridging atom, as discussed in Ref. [14]. The high reactivity of the bridging oxygen is claimed to be responsible for the capability of Fe/ZSM5 to oxidize NO to NO_2 and to decompose N_2O [1,8]. Noticeably, the presence of oxygen in the gas phase completely suppresses both the reduction of iron and the removal of the Fe–O–Fe bridging oxygen. The core structure of the binuclear complexes at 350 °C in oxygen ($P_{O_2} = 0.5$ bar) matches the model previously proposed by Chen and Sachtler [2].

In this paper the structure and the reactivity of the Fe-binuclear complexes in mildly calcined over-exchanged Fe/ZSM5 are studied under HC-SCR working conditions. This has been achieved by monitoring the local environment of the Fe-binuclear complexes at 350 °C: (i) in the presence of single HC-SCR reagents, i.e., NO, O_2, or i-C_4H_{10}, fed separately and (ii) during the HC-SCR reaction, i.e., in the contemporary presence of the three reagents. Information on the coordination geometry of Fe, obtained by the analysis of the Fe K-preedge features (centroid position and integrated intensity), has been used as input information for the fitting of the recorded EXAFS data. The catalytic activity of Fe/ZSM5 during the XAFS measurements has been monitored by analyzing the composition of the gas phase via a NO_x chemiluminescence analyzer.

2. Experimental

2.1. Catalyst preparation

NH_4/ZSM5 (Si/Al = 17.0, determined by ICP), obtained from Zeolyst, was converted into the acidic form by calcination in oxygen at 550 °C for 3 h. The resulting H/ZSM5 was used as host for the synthesis of over-exchanged Fe/ZSM5, by applying the $FeCl_3$ chemical vapor deposition technique [2]. The procedure applied has been described in detail previously [11,14]. First, anhydrous $FeCl_3$

was sublimated into the zeolite micropores. The sample was subsequently washed under stirring in doubly demineralized water for hydrolyzation and removal of excess chlorine. After drying overnight at 70 °C, the sample was calcined. The procedure applied (mild calcination) was identical to the one proposed in our previous work [11]. The sample was heated under a He flow of 800 ml/min with a moderate temperature ramp (0.5 °C/min) to 200 °C. At this temperature, 200 ml/min of O_2 were added to the He flow while, under the same temperature ramp, heating was continued to 550 °C. After 3 h at 550 °C, the temperature was decreased to 30 °C. The sample after calcination will be further denoted as Fe/ZSM5.

2.2. Catalytic testing

Fe/ZSM5 was tested for the selective catalytic reduction of NO with isobutane under plug-flow conditions. The catalyst (powder) was pressed, sieved to 90–212 µm, and charged in the reactor upon dilution with quartz. The sample was preheated to 350 °C with a rate of 5 °C/min under a He flow of 100 ml/min. The reaction feed was obtained by blending four flows, i.e., 1% NO/He, 1% i-C_4H_{10}/He, O_2, and He. Each flow rate was regulated by a digital Brooks mass-flow controller. The resulting inlet composition was 2000 vppm NO, 2000 vppm i-C_4H_{10}, 3 vol% O_2, balance He, with an overall flow of 140 ml/min. Catalytic tests were performed using 100 or 20 mg catalyst. Based on an apparent zeolite density of 0.5 g/cm^3, the calculated gas hourly space velocity (GHSV) was respectively 42,000 and 210,000 h^{-1}. The operating conditions applied during the activity tests are summarized in Table 1.

A Perkin-Elmer Autosystem XL gas chromatograph equipped with a TCD detector was used to monitor the effluent N_2, i-C_4H_{10}, N_2O, CO, and CO_2. The gases were separated using a Haysep Q and a Molsieve 13 X column (80–100 mesh). To measure NO and NO_2, a Thermo Environmental Instruments 42C NO_x chemiluminescence analyzer was connected in parallel to the gas chromatograph. The GC and the NO_x analyzer could be operated simultaneously. Catalytic data reported were measured after 60 min stabilization at each temperature.

Table 1
Description of the reactor and of the operating conditions during HC-SCR catalytic tests with isobutane on Fe/ZSM5

Parameters description	Test 1	Test 2
Catalyst amount (Fe/ZSM5) (mg)	100	20
Quartz amount (g)	4.0	0.45
Sieve fraction (µm)	90–212	90–212
Reactor internal diameter (mm)	12	4
Total bed length (mm)	36	25
Total feed rate (cm^3/min)	140	140
Calculated GHSV (h^{-1})	42,000	210,000

Feed composition (vol%): NO (0.2), i-C_4H_{10} (0.2), O_2 (3.0), balance He.

2.3. In situ Fe K-edge XAFS

2.3.1. XAFS data collection

The XAFS data were collected at the XI.1 measuring station at Hasylab (Hamburg, Germany). The experimental setup used is described in detail in Ref. [11]. Fe/ZSM5 was pressed to obtain self-supporting wafers, calculated to have a total absorption ($\mu \times x$) of 2.5, and placed in a controlled atmosphere cell [16]. Spectra were recorded after specific pretreatments. The complete list of the XAFS measurements, including detailed information on pretreatments, measuring conditions, and sample codes, is collected in Table 2. Fe/ZSM5 was heated to 350 °C under 50 ml/min flowing He (with the exception of measurement Fe/ZSM5-O_2 350/350, heated in the presence of oxygen). After 10 min stabilization at 350 °C, specific gas mixtures were fed to the cell, while the temperature was maintained at 350 °C. The composition of the different feeds is presented in Table 3. After 30 min on stream, three spectra were recorded in situ at 350 °C. After closing the in situ cell and cooling to 77 K, three additional scans were recorded. XANES spectra of hematite and Fe-titanate were also measured, upon purging with He at RT and cooling to 77 K. They were used, respectively, as internal Fe^{III} and Fe^{II} references. The three scans recorded for each measurement were compared and averaged, with the exception of the measurement Fe/ZSM5-He 350/350. As extensively discussed in Ref. [14], due to differences between the scans, caused by a partial reoxidation of the sample with time on stream, the three spectra of this measurement were not averaged. In this case, only data from the first scan were used.

2.3.2. Analysis of the Fe K preedge

The oxidation state of iron was determined by the analysis of the centroid position of the background subtracted Fe K preedge and by the position of the Fe K absorption edge. In addition, information on the local coordination geometry of iron was derived from the analysis of the preedge centroid position and of the background subtracted preedge integrated intensity [17]. The Fe K preedge was isolated from the XAFS spectra by using a cubic spline function, obtained by interpolating the data several electron volts before and after the preedge [14,17]. Centroid position and integrated intensity of the background-subtracted preedge were calculated with the software Grams. The estimated accuracy in the determination of the centroid position is ±0.1 eV. The error in the integrated intensity is approximately ±5%.

2.3.3. XAFS data processing

XAFS data were extracted from the measured absorption spectra by means of the XDAP code [18]. The preedge was subtracted using a modified Victoreen curve [19]. Background subtraction from the absorption XAFS spectra was performed by employing cubic spline routines, with a continuously adjustable smooth parameter [20,21]. Normaliza-

Table 2
List of XAFS spectra recorded from Fe/ZSM5: pretreatments and measuring conditions

Pretreatments (flowing atmosphere)	Environmental conditions during measurement	Measurements code
↑; He, 30 min at 350 °C	Flowing He, 350 °C	Fe/ZSM5-He 350/350
⤊; O_2/He, 60 min at 350 °C	Flowing O_2/He, 350 °C	Fe/ZSM5-O_2 350/350
↑; i-C_4H_{10}/He, 60 min at 350 °C	Flowing i-C_4H_{10}/He, 350 °C	Fe/ZSM5-CH_x 350/350
↑; i-C_4H_{10}/He, 90 min at 350 °C	i-C_4H_{10}/He, 77 K	Fe/ZSM5-CH_x 350/LN
↑; NO/He, 60 min at 350 °C	Flowing NO/He, 350 °C	Fe/ZSM5-NO 350/350
↑; NO/He, 90 min at 350 °C	NO/He, 77 K	Fe/ZSM5-NO 350/LN
↑; NO + O_2/He, 60 min at 350 °C	Flowing NO + O_2/He, 350 °C	Fe/ZSM5-NO + O_2 350/350
↑; NO + O_2/He, 90 min at 350 °C	NO + O_2/He, 77 K	Fe/ZSM5-NO + O_2 350/LN
↑; deNO/He, 60 min at 350 °C	Flowing deNO/He, 350 °C	Fe/ZSM5-deNO 350/350
↑; deNO/He, 90 min at 350 °C	deNO/He, 77 K	Fe/ZSM5-deNO 350/LN

↑, heating treatment to 350 °C (5 °C/min) performed in He. ⤊, heating treatment to 350 °C (5 °C/min) performed in O_2/He.

Table 3
Inlet gas composition during in situ XAFS measurements of Fe/ZSM5

Measurements code	Inlet gas composition (vol%)
Fe/ZSM5-He 350/350	He (100)
Fe/ZSM5-O_2 350/350	O_2 (50), balance He
Fe/ZSM5-CH_x 350/350	i-C_4H_{10} (0.2), balance He
Fe/ZSM5-NO 350/350	NO (0.2), balance He
Fe/ZSM5-NO + O_2 350/350	NO (0.2), O_2 (5), balance He
Fe/ZSM5-deNO 350/350	NO (0.2), i-C_4H_{10} (0.2), O_2 (5), balance He

tion was performed by dividing the data by the intensity of the absorption spectrum at 50 eV above the Fe K edge.

2.3.4. EXAFS data analysis, phase shifts, backscattering amplitudes

The local environment around iron, i.e., number and distances of Fe-neighboring atoms, was determined by EXAFS [20]. The information on the coordination geometry of Fe, obtained from the analysis of the Fe K preedge, was used as input for the EXAFS analysis.

The Fe–O reference was obtained from experimental EXAFS data of ferric acetylacetonate. The procedure followed for the creation of the Fe–O reference file is described in Ref. [11]. Fe–Fe phase shifts and backscattering amplitudes were calculated using the software FEFF7 [22]. The Fe–Fe reference was calibrated on EXAFS data obtained from hematite at 77 K [11], by fitting in R space. The crystallographic parameters used for the fit of the calibration reference [23,24] can be found in Ref. [11].

The EXAFS data analysis was performed by applying multiple-shell fitting in R space ($\Delta R = 0.7$–4.2 Å; $\Delta k = 2.7$–13.2 Å^{-1}). The difference file technique was applied together with phase-corrected Fourier transforms to resolve the different contributions in the EXAFS data [20]. The EXAFS fits were checked by applying k^1, k^2, and k^3 weightings.

The number of independent fit parameters (N_{indp}) was determined as outlined in Reports on Standard and Criteria in XAFS Spectroscopy [25]. For the measurements performed in this work it was calculated to be 25.4.

Errors in the numerical values obtained by the EXAFS data analysis are estimated to be ±10% in the coordination number (N), ±1% in the distance (R), ±5% in the Debye Waller factor ($\Delta\sigma^2$), and ±10% in the inner potential correction (ΔE_0) [26].

2.3.5. Catalytic activity during XAFS data collection

In order to measure the catalytic activity of Fe/ZSM5 during the collection of XAFS spectra Fe/ZSM5-NO 350/350, Fe/ZSM5-NO + O_2 350/350, and Fe/ZSM5-deNO 350/350 (see Table 2), a Thermo Environmental Instruments 42C NO_x chemiluminescence analyzer was connected in parallel to the outlet of the cell. The analyzer was calibrated independently for the detection of NO and NO_2. Concentrations of NO and NO_2 were measured at a time interval of 1 min, while recording the XAFS spectra. Stabilization of the NO and NO_2 concentration in the outlet was obtained for all the three measurements within 60 min from the beginning of the treatments.

Possible oxidation of NO to NO_2 occurring already at room temperature in the lines was monitored prior to and after the collection of the XAFS spectra Fe/ZSM5-NO 350/350, Fe/ZSM5-NO + O_2 350/350, and Fe/ZSM5-deNO 350/350. This was obtained by directly feeding the inlet gas to the NO_x analyzer via a bypass connected in parallel to the cell. The bypass was connected to the main line by means of two three-way valves, located at the inlet and at the outlet of the cell, respectively, and operated simultaneously. In all cases conversion of NO to NO_2 in the line was found to be below 0.4% with respect to the inlet concentration.

3. Results

3.1. HC-SCR catalytic testing

The results of the catalytic test performed on Fe/ZSM5 for the selective catalytic reduction of NO with isobutane under excess oxygen at 42,000 h^{-1} GHSV are depicted in Fig. 2a. Feed composition and GHSV for this test were chosen in order to be able to compare our results to the ones

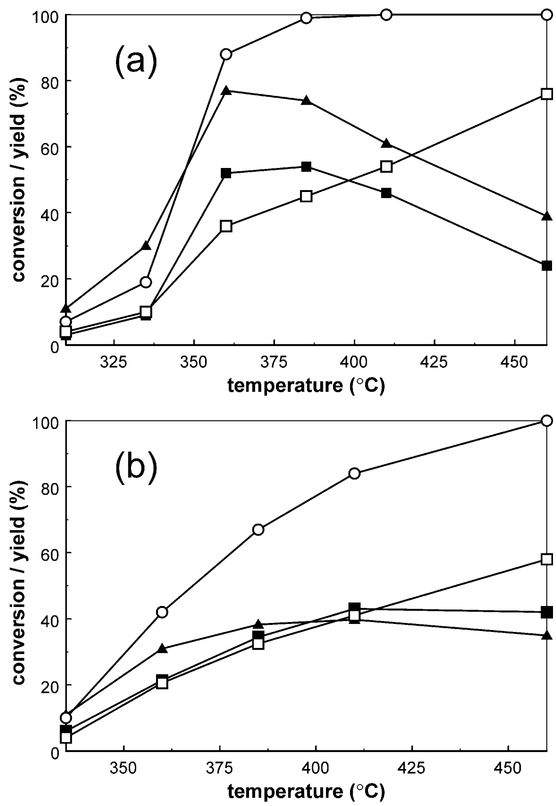

Fig. 2. Selective catalytic reduction of NO by isobutane over Fe/ZSM5 as a function of the reaction temperature: (▲) N_2 yield, (○) i-C_4H_{10} conversion, (■) i-C_4H_{10} conversion to CO, (□) i-C_4H_{10} conversion to CO_2. Inlet composition: 0.2% i-C_4H_{10} + 0.2% NO + 3% O_2, balance He. Total flow rate = 140 cm^3/min^{-1}. (a) GHSV = 42,000 h^{-1}; (b) GHSV = 210,000 h^{-1}. GHSV are based on an apparent zeolite density of 0.5 g/cm^{-3}.

already available in the literature [2]. In agreement with those results, a maximum in the conversion of NO to N_2 was obtained at a temperature of about 360 °C. The maximum N_2 yield was around 78%, confirming the high activity of Fe/ZSM5 toward the HC-SCR reaction, when using isobutane as reductant. Contemporarily, a considerable amount of CO (above 50% yield at maximum NO conversion) was formed, as a result of the incomplete i-C_4H_{10} combustion. Both N_2O and NO_2 were absent from the products, the selectivity toward N_2 being complete in the whole temperature range.

Reducing the residence time of the reactants (Fig. 2b, GHSV = 210,000 h^{-1}) caused a shift in the maximum N_2 yield toward higher temperature (to approximately 400 °C). Nevertheless, even under this extreme flow rate, the catalyst maintained a considerably high activity (around 36% maximum N_2 yield), while no N-containing by-products were detected in the gas phase.

3.2. Heat treatment in He and O_2

The normalized XANES spectra of Fe/ZSM5 recorded at 350 °C in He (Fe/ZSM5-He 350/350) (solid line) and in a 50/50 O_2/He mixture (Fe/ZSM5-O_2 350/350) (dotted line) are presented in Fig. 3a. The corresponding background-subtracted preedges are depicted in the upper-left part of the figure. XANES spectra measured from Fe-titanate and hematite are reported as internal references. As can be seen, the position of the Fe/ZSM5 Fe K edges are separated by approximately 4.0 eV. While the edge of the sample treated in oxygen corresponds to that of hematite (Fe^{III}), the edge of the sample measured in He appears to be close to that of Fe-titanate (Fe^{II}). The features of the preedges appear also to be different. The preedge measured in He is clearly shifted toward lower energy and displays a lower intensity.

Centroid position and integrated intensity of the preedge in Fe/ZSM5, measured upon the heat treatments, are plotted in Fig. 3b. In the same figure the Fe K preedge features of crystalline single-phase iron-containing references (large gray circles), obtained from the work of Wilke et al. [17], are reported for comparison. The Fe references differ for oxidation state (II or III) and for coordination geometry (from perfectly octahedral$^{(6)}$ to perfectly tetrahedral$^{(4)}$). The number in the upper brackets indicates the number of neighboring atoms in the Fe-coordination sphere. In the upper x axis of the figure the average oxidation state of iron (a.o.s.) is plotted as a function of the preedge centroid energy (lower x axis). This relation has been obtained by XAFS measurements on $^{(6)}Fe^{III}/^{(4)}Fe^{II}$ physical mixtures [17]. By comparison with the references, it can be concluded that the average oxidation state of iron in Fe/ZSM5 measured at 350 °C in He is close to 2.3+. Although only qualitative conclusions can be derived by the present data [14], the average Fe coordination in Fe/ZSM5 at 350 °C in helium appears to be close to that of fivefold or highly distorted tetrahedrally coordinated iron. Reduction of iron and oxygen removal from the Fe-coordination sphere, as already discussed in our previous work [14], are the result of auto-reduction phenomena occurring to Fe/ZSM5 during the heat treatment in the absence of oxygen. Iron in untreated Fe/ZSM5, indeed, is octahedrally coordinated, with an oxidation state of 3+ [11,14].

The oxidation state of iron in Fe/ZSM5 measured in the presence of oxygen at 350 °C is 3+. The Fe-coordination geometry corresponds to that of a fivefold coordinated reference. This shows that heating in oxygen influences the Fe–O coordination, decreased from six (untreated sample [14]) to five oxygen neighbors, but does not change the oxidation state of iron.

The differences in the Fe–O coordination sphere of Fe/ZSM5-He 350/350 and Fe/ZSM5-O_2 350/350 can be visualized by comparing the Fourier transforms of their EXAFS data (see Fig. 3c). The most distant peaks (Fe–Fe_1 and Fe–Fe_2) are due to Fe–Fe neighbors. As already discussed in our previous work [14], they are ascribed to the presence of binuclear Fe complexes, together with a minor fraction of Fe species with a higher Fe–Fe coordination. The main peak (Fe–O) is due to oxygen. As can be seen, this Fe–O peak in Fe/ZSM5-O_2 350/350 displays a higher intensity (real part) than in Fe/ZSM5-He 350/350. Furthermore the imaginary

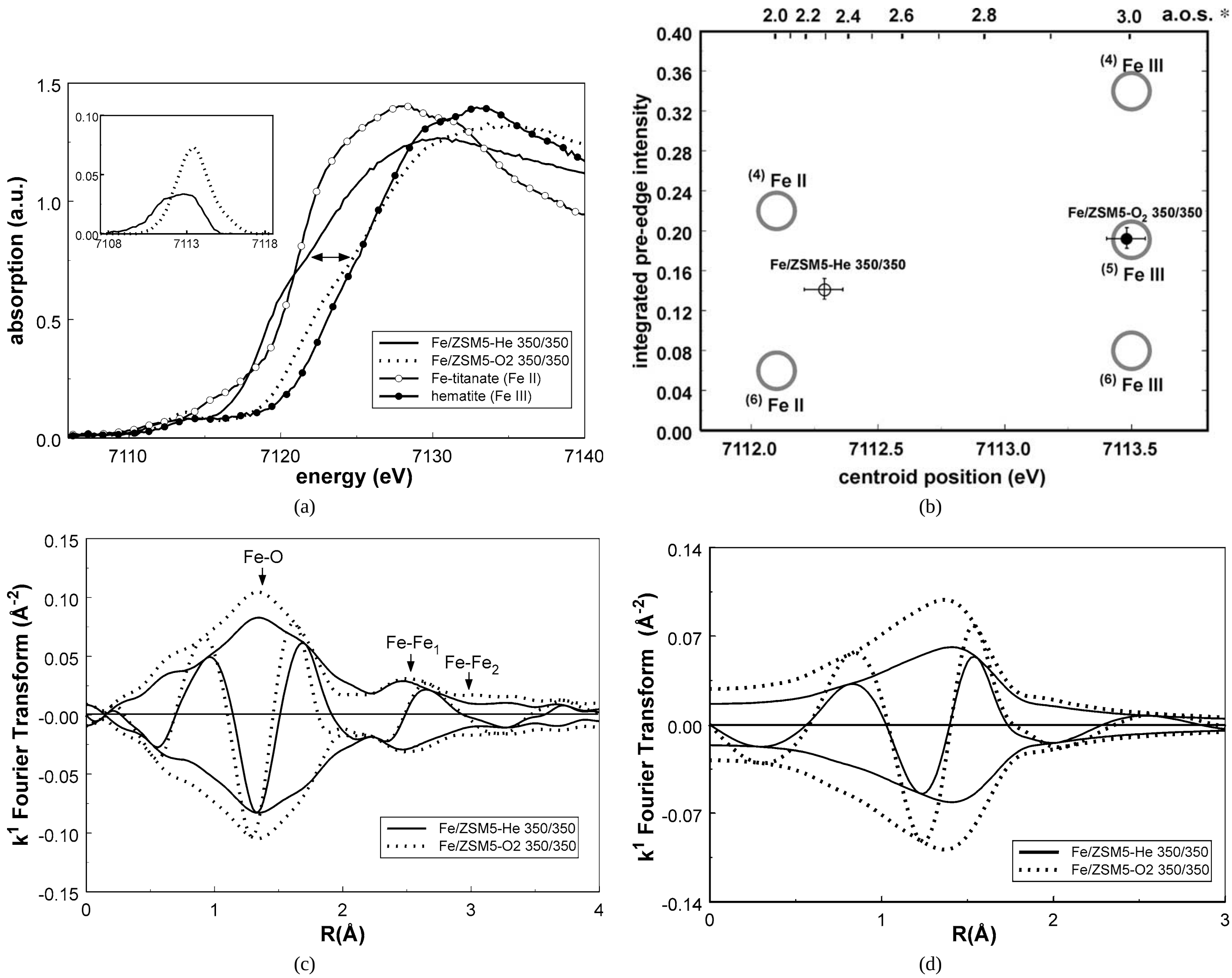

Fig. 3. (a) Normalized XANES spectra and background-subtracted preedges (enlarged in the upper-left part of the figure) of Fe/ZSM5-He 350/350 (solid line) and Fe/ZSM5-O_2 350/350 (dotted line). Normalized XANES spectra of hematite and Fe-titanate are also reported, respectively as internal Fe^{III} and Fe^{II} references. (b) Preedge characteristics (centroid position and integrated intensity) of Fe/ZSM5-He 350/350 (○) and Fe/ZSM5-O_2 350/350 (●). Preedge characteristics of iron with known coordination and oxidation state ($^{(6)}Fe^{III}$, $^{(5)}Fe^{III}$, $^{(4)}Fe^{III}$, $^{(6)}Fe^{II}$, $^{(4)}Fe^{II}$: (○)), obtained from the literature [17], are reported for comparison. * The average oxidation number (a.o.s.), reported in the upper x axis against the corresponding energy of the centroid positions (lower x axis), is based on experiments performed on $^{(6)}Fe^{III}/^{(4)}Fe^{II}$ binary mixtures with predetermined ratios. (c) Fourier transform (k^1, $\Delta k = 2.7$–13.2 Å^{-1}) of EXAFS data of Fe/ZSM5-He 350/350 (solid line) and Fe/ZSM5-O_2 350/350 (dotted line). (d) Fourier transform of the Fe–O_1 contribution obtained by R-space analysis (k^1, $\Delta k = 2.7$–13.2 Å^{-1}; $\Delta R = 0.7$–4.2 Å) of EXAFS data of Fe/ZSM5-He 350/350 (solid line) and Fe/ZSM5-O_2 350/350 (dotted line).

part appears to be clearly shifted toward lower distance. This indicates that in Fe/ZSM5-O_2 350/350 additional oxygen is present, located at low R.

The coordination parameters obtained by R-space analysis of the EXAFS data are presented in Table 4. For the fit, a distribution of oxygen in three different sub-shells was chosen. The assignment of three different Fe–O sub-shells was based on the results obtained during the heat treatments [14]. The model proposed for the evolution of the binuclear complexes upon heat treatments is shown in Fig. 1. Shell Fe–O_2, which remained unchanged, was ascribed to two oxygen atoms, anchoring the Fe atoms of the binuclear complexes to the Al-centered tetrahedra of the zeolite. The most distant O shell (Fe–O_3) could be attributed to a semibridging oxygen from the zeolite. Shell Fe–O_1 was attributed to a Fe–O–Fe bridging oxygen and to a terminal OH group. As can be seen, the most significant differences in the fit results for Fe/ZSM5-He 350/350 and Fe/ZSM5-O_2 350/350 are in shell Fe–O_1. Approximately two oxygen atoms (1.9) are present for Fe/ZSM5-O_2 350/350, while only 1.2 oxygen atoms are present for Fe/ZSM5-He 350/350. This difference can be explained by the removal of the bridging Fe–O–Fe oxygen, as a result of auto-reduction of iron at 350 °C in He. The clear differences in the Fe–O_1 shell as a function of the gas-phase composition can also be visualized qualitatively in Fig. 3d, where, for both measurements, the EXAFS Fourier transform of only contribution Fe–O_1 is plotted. As can be seen, the intensity of the shell in He appears to be almost halved. The presence of O_2 in the gas phase inhibits removal of oxygen.

Table 4
Coordination parameters obtained by R-space analysis (k^1, $\Delta k = 2.7$–13.2 Å^{-1}; $\Delta R = 0.7$–4.2 Å) of EXAFS data of Fe/ZSM5-He 350/350 and Fe/ZSM5-O_2 350/350; $N_{\text{indp}} = 25.4$; $N_{\text{free (fit)}} = 22$

Shells	N	R (Å)	$\Delta\sigma^2$ (10^{-3} Å^2)	ΔE_0 (eV)	k^1 variance (%)	
	±10%	±10%	±5%	±10%	Im. part	Abs. part
Fe/ZSM5-He 350/350					0.55	0.30
Fe–O_1	1.2	1.88	2.6	−5.5		
Fe–O_2	2.0	1.97	7.2	12.6		
Fe–O_3	1.2	2.08	8.8	−9.3		
Fe–Fe_1	1.1	2.99	13.0	0.4		
Fe–Fe_2	0.4	3.40	17.2	0.1		
Fe–O_Z	1.6	4.09	15.0	−8.8		
Fe/ZSM5-O_2 350/350					1.26	0.50
Fe–O_1	1.9	1.86	2.0	−2.5		
Fe–O_2	2.0	1.99	5.0	13.0		
Fe–O_3	1.0	2.02	1.6	−13.3		
Fe–Fe_1	1.2	2.99	9.8	−1.6		
Fe–Fe_2	0.4	3.40	15.1	−3.7		
Fe–O_Z	4.4	3.81	15.0	1.0		

The XANES spectra, the preedge features and the EXAFS results of the heat treatments in He and O_2 will be used as reference for the analysis of the XAFS data obtained in situ, during the separate feeding of i-C_4H_{10}, NO, and NO + O_2 and during the HC-SCR reaction with isobutane (see Tables 2 and 3).

3.3. Treatment with isobutane

The normalized XANES spectrum and the background-subtracted preedge of Fe/ZSM5 recorded at 350 °C in the presence of isobutane (Fe/ZSM5-CH_x 350/350, dashed line) is presented in Fig. 4a. The XANES spectra and preedges of Fe/ZSM5-He 350/350 (solid line) and of Fe/ZSM5-O_2 350/350 (dotted line) are also plotted, for comparison. Both the Fe K edge and the preedge of Fe/ZSM5-CH_x 350/350 appear to be similar to those measured at 350 °C in helium and only slightly shifted toward lower energy. This is ascribed to a minor additional reduction of Fe. The additional Fe reduction is confirmed by the analysis of the preedge features (Fig. 4b). The centroid position corresponds to an average iron oxidation state of 2.2.

In Fig. 4c the Fourier transform of the EXAFS data of measurement Fe/ZSM5-CH_x 350/350 (dotted line) is compared to that of Fe/ZSM5-He 350/350 (solid line). Differences are visible only in the 1.3–2.0 Å R range, where the real part of the sample treated with isobutane appears to be slightly enhanced. No differences are visible in the Fe–Fe coordination, showing no further aggregation of iron during the treatment. The Fourier transform of the EXAFS data of Fe/ZSM5-CH_x 350/350 (solid line) and the R-space fit (dotted line) are presented in Fig. 4d. It can be seen that the quality of the R-space fit is excellent. The coordination parameters obtained by the R-space analysis of the EXAFS data of Fe/ZSM5-CH_x 350/350 are presented in Table 5. In Fig. 4e the Fourier transform of shell Fe–O_1 is presented for measurements Fe/ZSM5-CH_x 350/350 (dashed line), Fe/ZSM5-He 350/350 (solid line) and Fe/ZSM5-O_2 350/350 (dotted line). As expected, in Fe/ZSM5 measured under isobutane this shell is significantly less intense than in the presence of oxygen. The intensity of the shell appears to be slightly lower than in the sample measured under He. The results confirm that the removal in a reducing atmosphere of oxygen is ascribable to the Fe–O–Fe bridges. They also demonstrate that almost all reactive oxygen from the sample can be removed by merely heating. A slight increase is visible in the coordination number of shell Fe–O_3 (from 1.2 to 1.4) when comparing the fit results of Fe/ZSM5-He 350/350 (Table 4) with those of Fe/ZSM5-CH_x 350/350 (Table 5). Since EXAFS in not able to distinguish between light-scattering atoms (in this study O, C, N), a precise assignment to the scattering neighbors is not possible. Nevertheless, it appears reasonable to ascribe the increase of the coordination number of shell Fe–O_3 to absorbed C-containing species.

Table 6 collects the coordination parameters of Fe/ZSM5, measured upon cooling the in situ cell to 77 K in the presence of the different reactants. A more severe increase in the coordination number of the Fe–O_3 shell (from $N = 1.4$ to 1.8), accompanied by a shift in its distance (from 2.08 to 2.14 Å), was detected upon cooling the sample under isobutane to 77 K. This can be explained by a further adsorption of C-containing species from isobutane, occurring during the cooling process.

3.4. Treatment with NO and NO + O_2

The catalytic activity of Fe/ZSM5 measured while recording the XAFS spectra of Fe/ZSM5-NO 350/350 and Fe/ZSM5-NO + O_2 350/350 is reported in Fig. 5. The conversion of NO is depicted by the black bars, while the corresponding NO_2 yield is depicted in white. Mass balance, calculated on nitrogen, showed that no measurable quantities of N_2 or N_2O were formed during the treatments. The concentration of the outlet gases reached a steady state after around 60 min from the beginning of the treatments and remained constant during the whole measurement. The delay in the stabilization is the result of back-mixing processes in the volume of the cell. As can be seen in Fig. 5 almost no activity was detected while flushing NO (2000 ppm) at 350 °C over Fe/ZSM5. A NO_2 yield lower than 1% was measured. This could be the result of oxidation of NO by traces of oxygen in the gas phase but is most probably due to inaccuracy in the NO_2 measurement. Clear oxidation of NO, on the other hand, was detected when feeding NO (2000 ppm) to the sample in the presence of oxygen (5%). A NO_2 yield of approximately 35% was obtained, as a result of the catalytic oxidation of NO by Fe/ZSM5.

The normalized XANES spectrum and the background-subtracted preedge of Fe/ZSM5-NO 350/350 (dashed line) and of Fe/ZSM5-NO + O_2 350/350 (dashed-dotted line) are presented in Fig. 6a. The XANES spectra and preedges

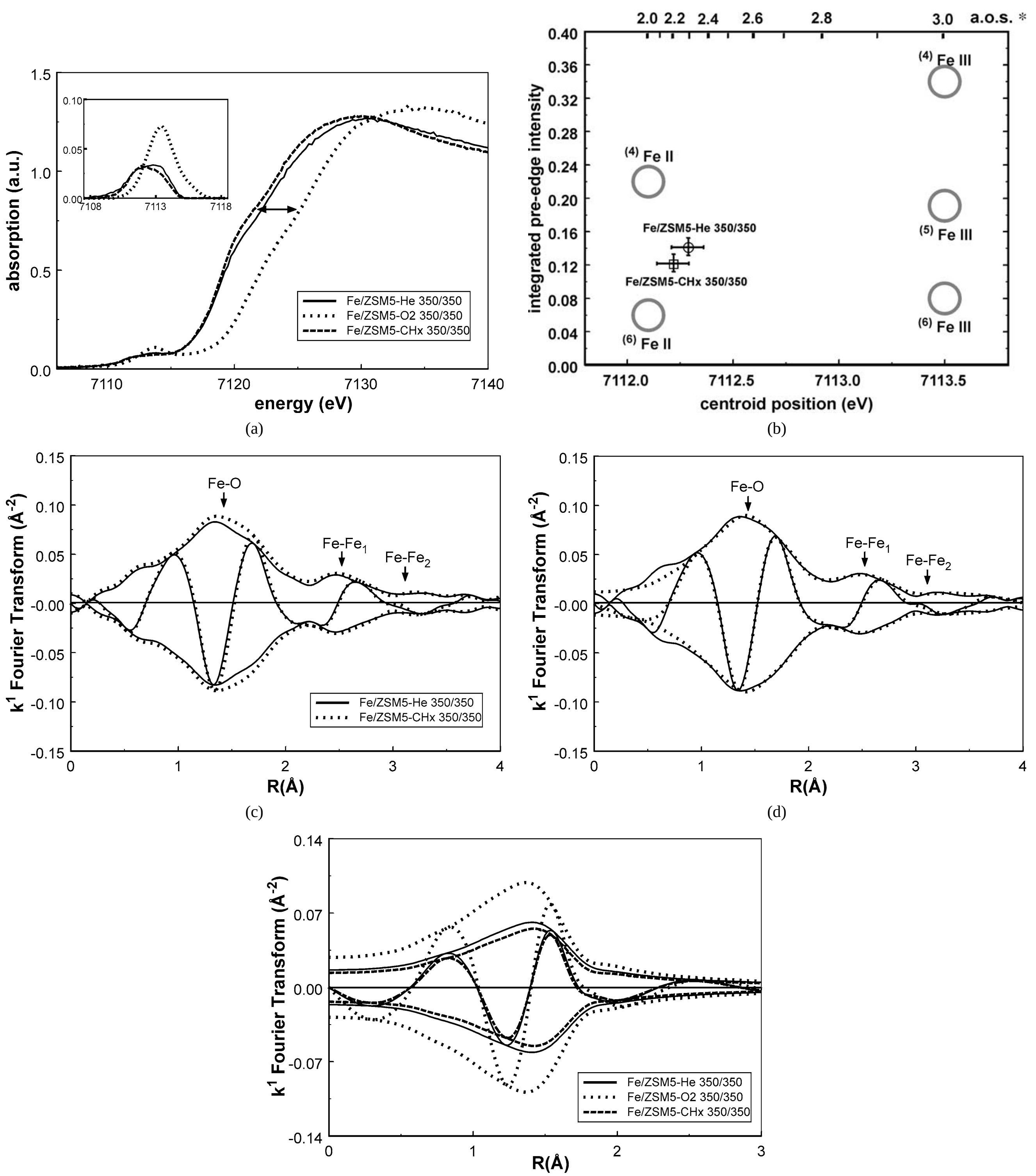

Fig. 4. (a) Normalized XANES spectra and background-subtracted preedges of Fe/ZSM5-CH$_x$ 350/350 (dashed line), Fe/ZSM5-He 350/350 (solid line), and Fe/ZSM5-O$_2$ 350/350 (dotted line). (b) Preedge characteristics (centroid position and integrated intensity) of Fe/ZSM5-CH$_x$ 350/350 (□) and of Fe/ZSM5-He 350/350 (○). For details on Fe references, see caption Fig. 3b. (c) Fourier transform (k^1, $\Delta k = 2.7$–13.2 Å^{-1}) of EXAFS data of Fe/ZSM5-CH$_x$ 350/350 (dotted line) and Fe/ZSM5-He 350/350 (solid line). (d) Fourier transform (k^1, $\Delta k = 2.7$–13.2 Å^{-1}) of EXAFS data of Fe/ZSM5-CH$_x$ 350/350 (solid line) and R-space fit (dotted line; $\Delta R = 0.7$–4.2 Å). (e) Fourier transform of the Fe–O$_1$ contribution obtained from the R-space analysis (k^1, $\Delta k = 2.7$–13.2 Å^{-1}; $\Delta R = 0.7$–4.2 Å) of EXAFS data of Fe/ZSM5-CH$_x$ 350/350 (dashed line), Fe/ZSM5-He 350/350 (solid line), and Fe/ZSM5-O$_2$ 350/350 (dotted line).

Table 5
Coordination parameters obtained by R-space analysis (k^1, $\Delta k = 2.7$–13.2 Å^{-1}; $\Delta R = 0.7$–4.2 Å) of EXAFS data of Fe/ZSM5-CH_x 350/350, Fe/ZSM5-NO 350/350, Fe/ZSM5-NO + O_2 350/350, and Fe/ZSM5-deNO 350/350; $N_{indp} = 25.4$; $N_{free\ (fit)} = 22$

Shells	N	R (Å)	$\Delta\sigma^2$ (10^{-3} Å^2)	ΔE_0 (eV)	k^1 variance (%)	
	±10%	±10%	±5%	±10%	Im. part	Abs. part
Fe/ZSM5-CH_x 350/350					0.36	0.27
Fe–O_1	1.0	1.88	0.8	−5.5		
Fe–O_2	2.0	1.97	8.4	12.6		
Fe–O_3	1.4	2.08	5.7	−9.2		
Fe–Fe_1	1.2	2.99	14.5	0.4		
Fe–Fe_2	0.4	3.40	17.2	0.1		
Fe–O_Z	1.7	4.09	15.0	−8.8		
Fe/ZSM5-NO 350/350					1.18	0.45
Fe–O_1	1.7	1.86	1.6	−1.5		
Fe–O_2	2.0	1.99	8.5	9.5		
Fe–O_3	1.0	2.02	0.5	−10.2		
Fe–Fe_1	1.2	3.00	8.9	−2.7		
Fe–Fe_2	0.4	3.40	15.0	−3.7		
Fe–O_Z	4.4	3.81	15.0	1.0		
Fe/ZSM5-NO + O_2 350/350					1.55	0.51
Fe–O_1	2.0	1.86	1.0	−6.9		
Fe–O_2	2.0	1.97	3.2	13.0		
Fe–O_3	1.0	2.02	1.0	−6.0		
Fe–Fe_1	1.2	2.96	10.5	1.9		
Fe–Fe_2	0.4	3.40	15.0	0.1		
Fe–O_Z	4.1	3.91	15.0	−2.2		
Fe/ZSM5-deNO 350/350					1.37	0.60
Fe–O_1	1.8	1.85	3.2	0.3		
Fe–O_2	2.0	1.97	6.0	13.0		
Fe–O_3	1.2	2.02	9.1	−12.1		
Fe–Fe_1	1.2	2.97	9.5	−0.2		
Fe–Fe_2	0.4	3.40	15.0	0.0		
Fe–O_Z	5.1	3.85	15.0	−0.4		

Table 6
Coordination parameters obtained by R-space analysis (k^1, $\Delta k = 2.7$–13.2 Å^{-1}; $\Delta R = 0.7$–4.2 Å) of EXAFS data of Fe/ZSM5-CH_x 350/LN, Fe/ZSM5-NO 350/LN, Fe/ZSM5-NO + O_2 350/LN, Fe/ZSM5-deNO 350/LN; $N_{indp} = 25.4$; $N_{free\ (fit)} = 22$

Shells	N	R (Å)	$\Delta\sigma^2$ (10^{-3} Å^2)	ΔE_0 (eV)	k^1 variance (%)	
	±10%	±10%	±5%	±10%	Im. part	Abs. part
Fe/ZSM5-CH_x 350/LN					0.45	0.22
Fe–O_1	1.0	1.85	−1.4	−0.4		
Fe–O_2	2.0	1.97	1.0	12.6		
Fe–O_3	1.8	2.14	9.5	−12.5		
Fe–Fe_1	1.2	2.99	3.8	1.1		
Fe–Fe_2	0.4	3.40	15.1	−6.6		
Fe–O_Z	2.7	4.02	15.0	3.1		
Fe/ZSM5-NO 350/LN					0.88	0.52
Fe–O_1	1.7	1.86	−3.5	−3.2		
Fe–O_2	2.0	1.99	−3.8	9.7		
Fe–O_3	1.2	2.09	8.7	−12.6		
Fe–Fe_1	1.2	3.00	1.6	−0.4		
Fe–Fe_2	0.4	3.40	15.0	−3.7		
Fe–O_Z	4.4	3.81	15.0	1.0		
Fe/ZSM5-NO + O_2 350/LN					0.66	0.30
Fe–O_1	2.0	1.85	−4.0	−4.0		
Fe–O_2	2.0	1.97	−5.0	13.0		
Fe–O_3	1.2	2.05	−1.2	−6.2		
Fe–Fe_1	1.2	2.98	3.1	2.0		
Fe–Fe_2	0.4	3.40	15.0	0.0		
Fe–O_Z	4.2	3.91	15.0	−2.2		
Fe/ZSM5-deNO 350/LN					0.80	0.60
Fe–O_1	2.0	1.85	−4.5	−0.7		
Fe–O_2	2.0	1.97	−5.0	13.0		
Fe–O_3	1.4	2.09	0.2	−6.3		
Fe–Fe_1	1.2	3.02	3.2	−2.7		
Fe–Fe_2	0.4	3.40	15.0	0.0		
Fe–O_Z	5.3	3.91	15.0	−2.2		

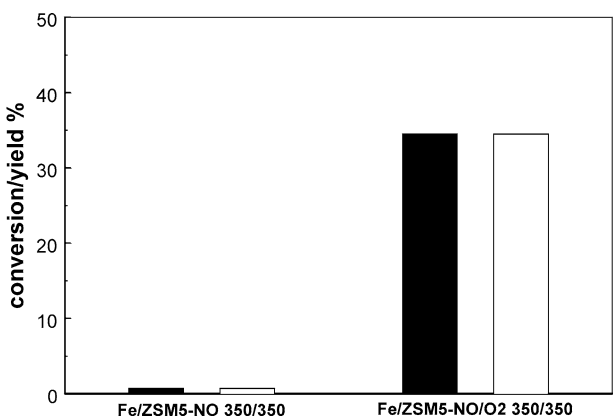

Fig. 5. NO conversion (black bars) and NO_2 yield (white bars), as detected by NO_x chemiluminescence analysis of the gas outlet, during in situ XAFS measurements of Fe/ZSM5-NO 350/350 and Fe/ZSM5-NO + O_2 350/350.

of Fe/ZSM5-He 350/350 (solid line) and of Fe/ZSM5-O_2 350/350 (dotted line) are included as references. The Fe K edge in the presence of NO and NO + O_2 appears to be positioned close to that measured in the presence of oxygen (Fe^{III}). They are separated by 0.4 eV, accounting for a slight average reduction of iron when NO was fed alone. No differences are visible when comparing the preedges of Fe/ZSM5-NO + O_2 350/350 and Fe/ZSM5-O_2 350/350. The preedge of Fe/ZSM5-NO 350/350, on the contrary, appears to be slightly less intense and shifted to lower energy. The preedge features are visualized in Fig. 6b. When NO is fed together with O_2, the features of iron in Fe/ZSM5 are typical of fivefold-coordinated Fe^{III}. A similar coordination is measured in the absence of oxygen (Fe/ZSM5-NO 350/350), together with an average oxidation number of 2.8–2.9.

The Fourier transform of the EXAFS data of Fe/ZSM5-NO 350/350 and Fe/ZSM5-NO + O_2 350/350 is reported in Fig. 6c. As can be seen, the total Fe–O coordination of both measurements overlaps with that of Fe/ZSM5-O_2 350/350. The imaginary part of Fe/ZSM5-NO 350/350 in the R range 1.0–2.0 Å appears only slightly shifted to higher distance when compared to that of Fe/ZSM5-NO + O_2 350/350. The structural parameters obtained by the analysis of the EXAFS data, measured at 350 °C and LN temperature, are presented in Tables 5 and 6, respectively. Measurements

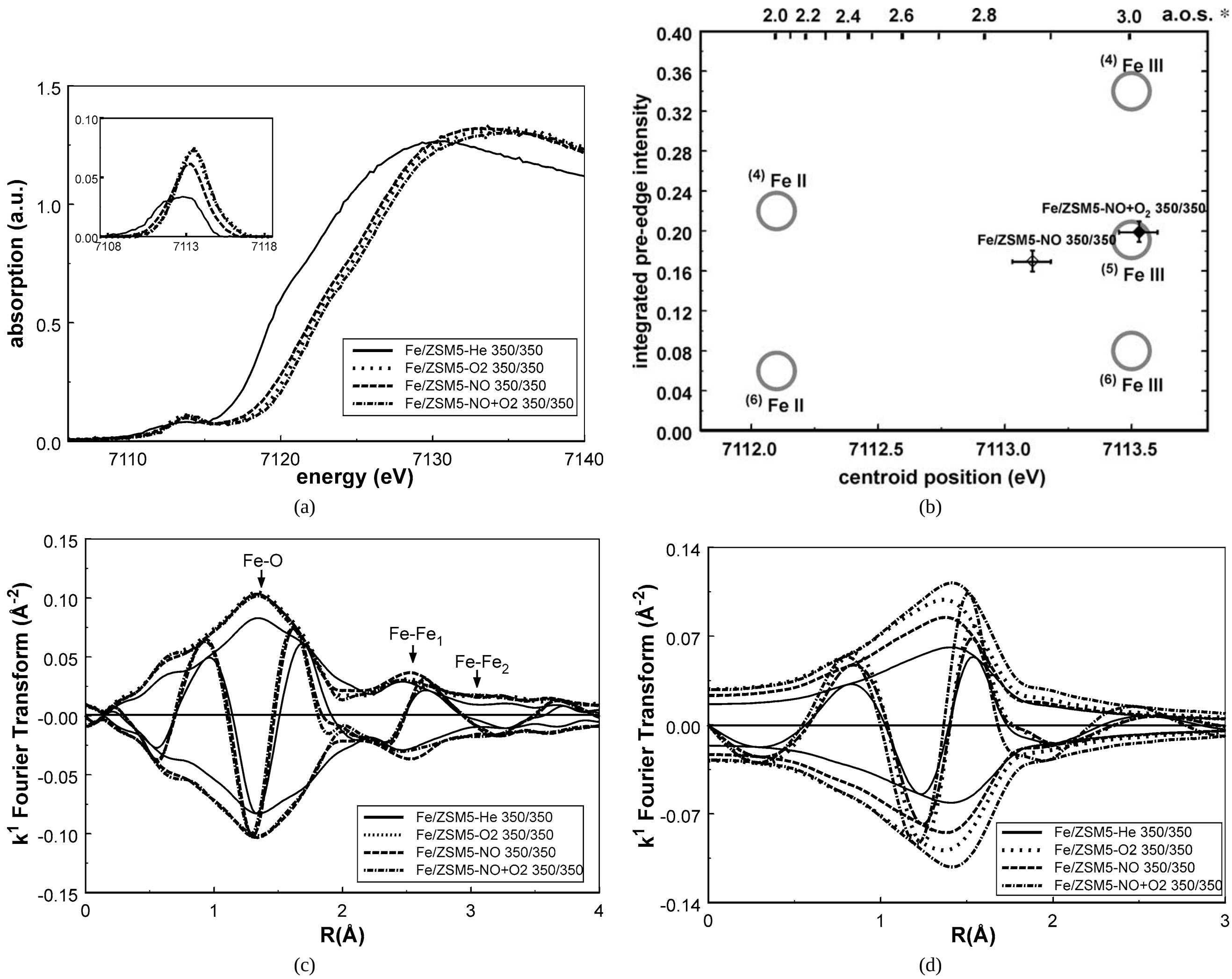

Fig. 6. (a) Normalized XANES spectra and background-subtracted preedges of Fe/ZSM5-NO 350/350 (dashed line), Fe/ZSM5-NO + O_2 350/350 (dashed-dotted line), Fe/ZSM5-He 350/350 (solid line), and Fe/ZSM5-O_2 350/350 (dotted line). (b) Preedge characteristics (centroid position and integrated intensity) of Fe/ZSM5-NO 350/350 (◇) and Fe/ZSM5-NO + O_2 350/350 (◆). For details on Fe references, see caption to Fig. 3b. (c) Fourier transform (k^1, $\Delta k = 2.7$–13.2 Å^{-1}) of EXAFS data of Fe/ZSM5-NO 350/350 (dashed line), Fe/ZSM5-NO + O_2 350/350 (dashed-dotted line), Fe/ZSM5-He 350/350 (solid line), and Fe/ZSM5-O_2 350/350 (dotted line). (d) Fourier transform of the Fe–O_1 contribution obtained by R-space analysis (k^1, $\Delta k = 2.7$–13.2 Å^{-1}; $\Delta R = 0.7$–4.2 Å) of EXAFS data of Fe/ZSM5-NO 350/350 (dashed line), Fe/ZSM5-NO + O_2 350/350 (dashed-dotted line), Fe/ZSM5-He 350/350 (solid line), and Fe/ZSM5-O_2 350/350 (dotted line).

Fe/ZSM5-NO 350/350 and Fe/ZSM5-NO + O_2 350/350 show a total Fe–O coordination of 4.7 and 5.0, respectively. Differences between the two measurements are visible in the coordination number of the closest shell (Fe–O_1), showing the presence on average of 1.7 (Fe/ZSM5-NO 350/350) or 2.0 (Fe/ZSM5-NO + O_2 350/350) neighbors. Similar coordination numbers have been obtained for the same measurements upon cooling to LN temperature.

The Fourier transforms of the EXAFS function of the closest Fe–O shell (Fe–O_1) are shown in Fig. 6d. Differences are visible between the intensities of the real part of the Fourier transforms. The intensities are in the order Fe/ZSM5-NO 350/350 < Fe/ZSM5-O_2 350/350 < Fe/ZSM5-NO + O_2 350/350.

3.5. SCR of NO with isobutane

The catalytic activity of the Fe/ZSM5 sample towards the HC-SCR reaction of NO with isobutane was monitored during the collection of the XAFS data of measurement Fe/ZSM5-deNO 350/350. A complete stabilization of the composition of the outlet gas was obtained upon approximately 60 min under reaction. The outlet composition remained stable during the recording of the XAFS spectra. The catalytic results are shown in Fig. 7. The conversion of NO is indicated by the black bar, while the NO_2 yield is depicted in white. The N_2 yield (gray bar) was calculated by mass balance on nitrogen, by assuming no formation of N_2O. Indeed, as shown in Figs. 2a and 2b, N_2O is not a by-product

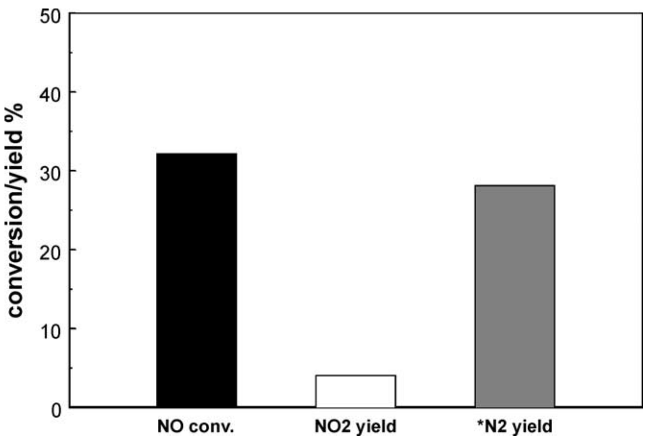

Fig. 7. NO conversion (black bar), NO_2 yield (white bar), and N_2 yield (dark-gray bar), as detected by NO_x chemiluminescence analysis of the gas outlet, during in situ XAFS measurements of Fe/ZSM5-deNO 350/350. *N_2 yield is calculated from mass balance on nitrogen, assuming no formation of N-containing products different from NO and NO_2.

of HC-SCR with isobutane on Fe/ZSM5. Furthermore, the reproducibility of the catalytic results was confirmed by subsequent catalytic tests performed in the in situ XAFS cell, by measuring N_2 directly by gas chromatography. As can be see in Fig. 7, a NO conversion of 32% could be obtained. This result demonstrates that the XAFS spectra were obtained from the catalyst under deNO_x working conditions. Together with N_2 (28% yield) also the formation of a minor amount of NO_2 was detected (4% yield). Since NO_2 is not a by-product of the HC-SCR reaction catalyzed by Fe/ZSM5, its formation was most probably the result of oxidation of NO by oxygen, occurring on the stainless-steel walls of the cell or in the gas phase.

The normalized XANES spectrum and the background-subtracted preedge of Fe/ZSM5 recorded at 350 °C during the SCR reaction of NO by isobutane (Fe/ZSM5-deNO 350/350, dashed line) are presented in Fig. 8a and compared with those of Fe/ZSM5-He 350/350 (solid line) and of Fe/ZSM5-O_2 350/350 (dotted line). The position of the Fe K edge shows that the average oxidation state of iron in Fe/ZSM5 during reaction is 3+. The intensity of the preedge of Fe/ZSM5-deNO 350/350 appears to be lower than that measured at 350 °C in oxygen. This can be ascribed to the presence of reaction intermediates in the coordination of iron. The analysis of the preedge features, presented in Fig. 8b, confirms that the oxidation state of iron during reaction is 3+. The integrated preedge intensity is consistent with the presence on average of 5 to 6 neighboring atoms.

The Fourier transform of the EXAFS data of Fe/ZSM5-deNO 350/350 is shown in Fig. 8c. As in the case of separate feeding of NO or NO + O_2 (Fig. 6c), the Fourier transform appears similar to that of measurement Fe/ZSM5-O_2 350/350. The EXAFS data analysis (Table 5) shows that the coordination number of the Fe–O_1 shell is slightly reduced, from 2.0 to 1.8. The Fourier transform of the EXAFS function of the Fe–O_1 contribution (plotted in Fig. 8d) shows indeed a slight decrease in the intensity of the real part. This may indicate a slight removal of oxygen from the Fe–O–Fe bridges. Due to the contemporary presence of chemically different light scatterers, attribution to specific neighbors is not possible. It should furthermore be noted that the slight decrease in intensity in the Fe–O_1 contribution is not accompanied by a reduction of iron.

Cooling to LN temperature resulted in an average increase in the number of neighbors in the closest Fe coordination (Fe/ZSM5-deNO 350/LN, Table 6), ascribed to further adsorption at low temperature. The coordination number of shell Fe–O_1 appeared to be slightly increased, from 1.8 to 2.0 neighbors. Also the coordination of shell Fe–O_3, previously attributed to adsorbed water [14], appeared to be enhanced (from 1.2 to 1.4). This may be the result of adsorption, upon cooling, of water produced during the HC-SCR reaction, but could as well be caused by the presence of C/N-containing reaction-intermediates.

4. Discussion

4.1. Catalytic activity of Fe/ZSM5 toward SCR of NO with isobutane

The catalytic tests performed on the Fe/ZSM5 sample, further used for the in situ XAFS characterization, confirm the high activity and selectivity of this catalyst for the selective catalytic reduction of NO to N_2 with isobutane (Figs. 2a and 2b). The performance of our sample appears to be identical to that shown by previous studies [2–5]. A maximum N_2 yield can be obtained at around 360 °C (around 78% at a GHSV of 42,000 h^{-1}), the selectivity toward N_2 being complete. Reducing the contact time of the reactants by five times (GHSV = 210,000 h^{-1}) does not result in a corresponding decrease in activity. Even under this extremely high flow rate, Fe/ZSM5 still provides a N_2 yield of around 36% (Fig. 2b), coupled by a complete selectivity toward N_2. While these results appear very promising for practical applications of Fe/ZSM5, further tests are needed. In particular, the stability of the catalyst should be established under more realistic conditions, i.e., in the presence of water. As shown in our previous work [11], the presence of water at high temperature can be responsible for aggregation of iron and formation of unreactive hematite crystals on the external surface of the zeolite. This phenomenon could result in severe deactivation of the catalyst with time on stream.

4.2. Structure of the Fe-binuclear complexes and reactivity during heat treatment in He and O_2

XAFS spectroscopy allowed us to describe the structure of the Fe-binuclear complexes in Fe/ZSM5, prepared by sublimation of $FeCl_3$. This was achieved by studying a sample calcined with a controlled procedure, aimed at minimizing the formation of (inactive) spectators [11,14]. It was also

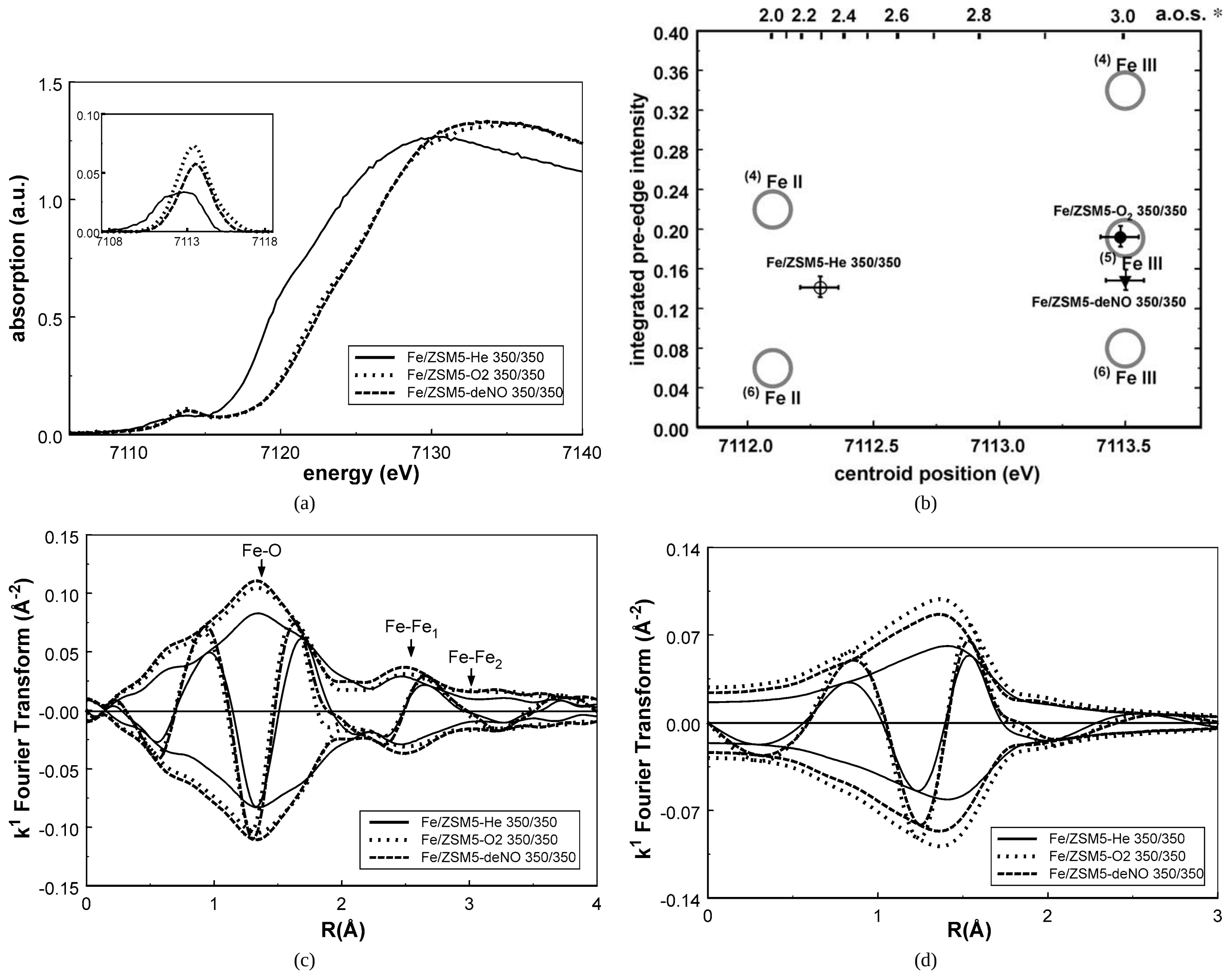

Fig. 8. (a) Normalized XANES spectra and background-subtracted preedges of Fe/ZSM5-deNO 350/350 (dashed line), Fe/ZSM5-He 350/350 (solid line), and Fe/ZSM5-O_2 350/350 (dotted line). (b) Preedge characteristics (centroid position and integrated intensity) of Fe/ZSM5-deNO 350/350 (▼), Fe/ZSM5-He 350/350 (○), and Fe/ZSM5-O_2 350/350 (●). For details on Fe references, see caption to Fig. 3b. (c) Fourier transform (k^1, $\Delta k = 2.7$–13.2 Å^{-1}) of EXAFS data of Fe/ZSM5-deNO 350/350 (dashed line), Fe/ZSM5-He 350/350 (solid line), and Fe/ZSM5-O_2 350/350 (dotted line). (d) Fourier transform of the Fe–O_1 contribution obtained by R-space analysis (k^1, $\Delta k = 2.7$–13.2 Å^{-1}; $\Delta R = 0.7$–4.2 Å) of EXAFS data of Fe/ZSM5-deNO 350/350 (dashed line), Fe/ZSM5-He 350/350 (solid line), and Fe/ZSM5-O_2 350/350 (dotted line).

possible, as shown in a previous paper [14], to rationalize the reactivity of the Fe-binuclear clusters during heat treatments in He and O_2 (see Fig. 1). The reactivity of oxygen in the complexes has been identified in the Fe–O_1 and Fe–O_3 shells located in the R range (1.85–1.89 Å) and (2.02–2.09 Å), respectively. Shell Fe–O_2 (1.97–1.99 Å), which remained unmodified during the treatments, has been ascribed to oxygen from the aluminum-centered tetrahedra, anchoring the Fe atoms to the framework of the zeolite. Removal of one oxygen atom from shell Fe–O_3 occurs already at low temperature ($\sim 150\,^{\circ}$C) and does not affect the oxidation state of iron. This has therefore been assigned to desorption of water. Shell Fe–O_1, on the contrary, appears to be affected only at higher temperatures (above $250\,^{\circ}$C) and is strongly influenced by the composition of the gas phase. Approximately one oxygen atom can be removed, and only in the complete absence of oxygen from the gas phase. Removal of this oxygen results, in reduction of iron. The reactivity of this shell has been ascribed to the presence of highly reactive Fe–O–Fe bridges in the Fe-binuclear complexes. This background information will be used as a basis for a further investigation of the active coordination site(s) of the binuclear Fe complexes. The influence of the different reactants on these coordination sites will be discussed.

4.3. *Treatment with isobutane*

Fe/ZSM5 was treated with isobutane upon heating to $350\,^{\circ}$C in He. The influence of isobutane on the binuclear Fe complexes can therefore be tracked by comparing the results obtained by measurements Fe/ZSM5-CH_x 350/350 and Fe/ZSM5-He 350/350. The average oxidation state of iron for the two measurements appear similar, being respectively around 2.2 and 2.3 (Figs. 4a and 4b). It can therefore be concluded that treating with isobutane results in only a slight further reduction of iron, when compared to that caused by heating in He to 350 °C (auto-reduction). Thus, the majority of reactive oxygen can be activated and desorbed from the Fe-binuclear complexes by merely heating. The slight increase in the reduction upon reaction with isobutane corresponds to a further removal of oxygen from the closest Fe–O shell (Fe–O_1), as shown by the decrease of its coordination number (from 1.2 in Fe/ZSM5-He 350/350 to 1.0 in Fe/ZSM5-CH_x 350/350, Tables 4 and 5). It is therefore ascribed to the extraction of oxygen from the Fe–O–Fe bridges. The slight decrease in the preedge intensity (Fig. 4b), together with the increase in the coordination number of shell Fe–O_3, suggests the presence on iron of C-containing adsorbed species from isobutane. After cooling to LN temperature, the coordination number of shell Fe–O_3 increased significantly (Tables 5 and 6), as a result of further adsorption resulting from the cooling. The treatment in i-C_4H_{10} did not cause any change in shell Fe–O_2, attributed to oxygen in Fe–O–Al bridges (see Fig. 1). This shows that the Fe complexes remained firmly ligated to the zeolite framework. Indeed, no increase was visible in the Fe–Fe coordination, demonstrating that no further aggregation phenomena of iron occurred during the treatment.

4.4. *Treatment with NO and NO + O_2*

The catalytic measurements performed during the collection of the XAFS spectra of Fe/ZSM5-NO 350/350 do not show any detectable activity for the catalytic decomposition of NO by Fe/ZSM5 (Fig. 5).

Flushing NO results in a clear increase in the oxidation state of iron, from 2.3 (Fe/ZSM5-He 350/350, Fig. 3b) to approximately 2.8–2.9 (Fig. 6b). The reason for the reoxidation could be manifold. As shown in our previous work [14] reduced Fe-binuclear complexes are highly unstable. Indeed, partial reoxidation of the complexes was detected with time on stream under He. Voskoboinikov et al. [7] suggested the possibility of oxygen exchangeability between the Fe complexes and the zeolite matrix. Reoxidation could have therefore been caused by extraction of oxygen from the zeolite lattice. Traces of oxygen in the gas phase may also have been responsible for the reoxidation. Indeed, as previously demonstrated [14], the oxygen vacancy between the two iron ions is readily regenerated by molecular oxygen from the gas phase. Nevertheless, oxidation by oxygen is not the only possible explanation. Fu et al. [27] have shown that NO can act as an oxidant in Fe/Y, where also the presence of binuclear Fe complexes has been suggested. Lei et al. [28] have demonstrated that on $[Cu–O–Cu]^{2+}$ ions in Cu/ZSM5 the same phenomenon occurs by the interaction of two NO molecules and the generation of one molecule of N_2O. The same pathway may occur on the Fe-binuclear complexes in Fe/ZSM5:

$$\begin{aligned}&2\mathrm{NO} + \left[\mathrm{HO{-}Fe^{2+}{-}\square{-}Fe^{2+}{-}OH}\right]\\&\quad\rightarrow \left[\mathrm{HO{-}Fe^{3+}{-}O{-}Fe^{3+}{-}OH}\right] + \mathrm{N_2O}\uparrow,\end{aligned}\tag{1}$$

where □ stands for a vacancy. The N_2O formed, present in negligible concentration in the gas outlet, could not have been detected by our gas-analysis system.

Contemporarily with the reoxidation of iron, an increase was visible in the number of Fe-neighboring atoms in the Fe–O_1 shell (from 1.2 in Fe/ZSM5-He 350/350 to 1.7 in Fe/ZSM5-NO 350/350). When compared to the measurement performed in the presence of oxygen, the shell was not completely regenerated (1.7 neighbors for Fe/ZSM5-NO 350/350 against 1.9 for Fe/ZSM5-O_2 350/350). As previously discussed, EXAFS is not able to distinguish between different light-scattering atoms (O or N). The neighboring atoms in shell Fe–O_1 could therefore be attributed to oxygen (partial regeneration of Fe–O–Fe bridges) or to the presence of N-containing adsorbed species. Several FTIR studies have been performed to identify the species formed by the interaction of NO with the active sites of iron catalysts [3,4,6,8,13, 29–33]. Chen et al. [8], in particular, have studied the evolution of the N-containing adsorbed species generated by NO on over-exchanged Fe/ZSM5, obtained by chemical vapor deposition of $FeCl_3$. From their study different species have been identified as nitrosyl $Fe^{n+}(NO)_{1,2}$ and $Fe^{n+}(NO_2)$, the latter being formed with increasing time on stream.

These species, which tend to be formed more easily on reduced iron (Fe^{2+}) (2), may exist as well on Fe^{3+} [34] (3):

$$\begin{aligned}&2\mathrm{NO} + \left[\mathrm{HO{-}Fe^{2+}{-}\square{-}Fe^{2+}{-}OH}\right]\\&\quad\rightarrow \left[\mathrm{HO{-}\overset{\substack{O\\|\\N\\|}}{Fe^{2+}}{-}\square{-}\overset{\substack{O\\|\\N\\|}}{Fe^{2+}}{-}OH}\right],\end{aligned}\tag{2}$$

$$\begin{aligned}&2\mathrm{NO} + \left[\mathrm{HO{-}Fe^{3+}{-}O{-}Fe^{3+}{-}OH}\right]\\&\quad\rightarrow \left[\mathrm{HO{-}\overset{\substack{O\\|\\N\\|}}{Fe^{3+}}{-}O{-}\overset{\substack{O\\|\\N\\|}}{Fe^{3+}}{-}OH}\right].\end{aligned}\tag{3}$$

Fe^{3+}, as previously discussed, may have been generated by reoxidation with oxygen, or by NO, following pathway (1).

Together with the partial regeneration of the Fe–O–Fe bridges, via the pathway proposed by Lei et al. [28], nitrosyl species appear to be the most probable responsible for the changes affecting the closest coordination of iron (Fe–O_1) under NO at 350 °C.

While Fe/ZSM5 is not able to decompose NO to N_2 and O_2, it is an active catalyst for the oxidation of NO to NO_2 in the presence of excess oxygen (see Fig. 5). The capability of Fe/ZSM5 to oxidize NO to NO_2 is well known. Catalytic tests performed by Chen et al. [8], using a feed composition similar to the one used in this work, showed a maximum conversion of NO to NO_2 of around 75% at 300 °C under a GHSV of 42,000 h^{-1}. As suggested by the authors, NO_2 is most likely formed by the reaction of NO with the bridging oxygen in Fe–O–Fe. The vacancy generated should be reoccupied by oxygen from the gas phase, or possibly by

NO, following pathway (1). FTIR studies [8,31] have shown that prevalently nitro $(NO_2)^-$ and nitrate $(NO_3)^-$ species are formed when NO and O_2 are fed together on Fe/ZSM5. Different pathways have been suggested for the formation of these species. Lobree et al. [31] have proposed, as the first step in this process, the formation of a superoxide ion $(O_2)^-$, generated by the reaction of O_2 with the Fe complexes, followed by a disproportionation of the iron atoms in the Fe complexes, with the formation of a [HO–Fe^{2+}] and a [$O_2{}^-$–Fe^{3+}–OH] group. Nitrate and nitro species should be formed by the subsequent reaction of NO and NO_2 from the gas phase, respectively with the [$O_2{}^-$–Fe^{3+}–OH] and the [HO–Fe^{2+}] groups. Chen et al. [8] have proposed a different pathway, via the formation of a peroxo bridge between the two Fe atoms in the complexes. The reaction of NO and NO_2 with the highly unstable peroxo group would generate the nitro and nitrate species.

The immediate reoxidation of iron (Fig. 6a) occurred upon contemporarily purging of NO and O_2 shows that, indeed, the Fe-binuclear complexes in Fe/ZSM5 are highly reactivity towards this mixture. The oxidation state of iron appears to be somewhat higher than that measured in the presence of NO alone. This observation, coupled with the increase in the coordination number of shell Fe–O_1, which appears almost identical to that measured in the presence of oxygen alone (Fe/ZSM5-O_2 350/350), suggests a complete regeneration of the Fe–O–Fe bridges. The possible formation of highly unstable peroxo bridges, suggested by Chen et al. [8] could not have been detected by the EXAFS setup used in this study. It should be noted that the increment in the coordination number of shell Fe–O_1 could also be assigned to the presence of absorbed nitro and nitrate species. A clear assignment with the present data is not possible.

As in the case of the treatment with isobutane and NO, also in the contemporary presence of NO and O_2 no significant changes were detected in shell Fe–O_2, attributed to oxygen binding the Fe complexes to the zeolite framework, nor in the Fe–Fe coordination. It can be concluded that also in the presence of NO and NO + O_2 the binuclear complexes remained stably ligated to the framework and that no agglomeration of iron toward larger clusters occurred.

4.5. SCR of NO with isobutane

The activity of Fe/ZSM5 towards the selective catalytic reduction of NO to N_2 with isobutane was confirmed by the analysis of the outlet gases (Fig. 7), performed during the collection of the XAFS spectra Fe/ZSM5-deNO 350/350. The gas analysis shows that the XAFS spectra were recorded on Fe/ZSM5 under deNO working conditions.

As in the case of the treatments with NO or NO + O_2, changes occurring upon reaction with the HC-SCR mixture were identified in the closest Fe–O coordination sphere of the complexes. The coordination number of shell Fe–O_1 ($N = 1.8$) appeared to be significantly increased when compared to the sample heated in He ($N = 1.2$). This was accompanied by a complete reoxidation of iron (Fe^{3+}). This result confirms that the reactivity of the Fe complexes originates in the oxygen vacancies formed upon heating. Due to the inability of EXAFS to distinguish between light scatterers of different nature (C, N, O), it is not possible to assign the changes in the Fe–O_1 coordination to an interaction with a specific reactant. As previously observed, the increase in the coordination number of shell Fe–O_1 can in principle be ascribed to the regeneration of the Fe–O–Fe bridges, operated by O_2 or by NO/NO_2 from the gas phase, following pathway (2). Nevertheless, the reaction pathway for the HC-SCR reaction, elucidated by Chen et al. [3,4] and Gao et al. [6], and presented in the introduction, shows that an extremely wide range of reaction intermediates may coexist on the binuclear Fe complexes during reaction. The most plausible candidates consist of organic nitro and nitroso compounds. The presence during the SCR reaction of different adsorbed species in the coordination sphere of iron is confirmed by the large increase detected in the static disorder in the most distant Fe–O shell of the Fe complexes (Fe–O_3), and by the lowered intensity of the Fe preedge when compared to that measured in the presence of oxygen alone (Fig. 8b). The intensity of the preedge appears to be consistent with the presence of five to six atomic neighbors. Coherently, 5.0 neighbors were found by the EXAFS analysis. It should nevertheless be noted that, due to the extremely high static disorder originated by the different reaction intermediates, this number could be slightly underestimated. Indeed, upon cooling to 77 K, a slight increase was detected in the coordination number of shells Fe–O_1 and Fe–O_3. The increase in the coordination number of shell Fe–O_3, in particular, could be attributed as well to adsorption at low temperature of water produced by combustion of isobutane during reaction.

5. Conclusions

The majority of iron in Fe/ZSM5 obtained by sublimation of $FeCl_3$, and calcined by using a special procedure aimed at minimizing the number of (inactive) Fe spectators, consists of oxo/hydroxo binuclear Fe complexes with a Fe–O–Fe core.

During heat treatment in He to 350 °C the Fe complexes undergo auto-reduction. This is ascribed to removal of oxygen from the Fe–O–Fe bridges (closest Fe–O coordination sphere), with the consequent formation of Fe–□–Fe vacancies.

The majority of reactive oxygen can be activated and desorbed from the Fe-binuclear complexes by merely heating. Treatment with isobutane results in only a further slight (average) reduction of iron, accompanied by an additional removal of oxygen from the Fe–O–Fe bridges.

The active sites of the Fe complexes are located in the vacancies generated in the closest Fe–O coordination sphere by the oxygen desorption. Upon reaction with NO and

$NO + O_2$ these vacancies are promptly reoccupied and iron is oxidized. This can be ascribed to the regeneration of the Fe–O–Fe bridges in the complexes, possibly accompanied by adsorption of N-containing species.

Also during HC-SCR conditions the closest Fe–O shell is reoccupied, leading to reoxidation of Fe (Fe^{3+}). Contemporarily, a large increase is detected in the static disorder in the most distant Fe–O shell of the Fe complexes. This suggests that adsorbates (HC-SCR reaction intermediates) are formed on these sites. No conclusions can nevertheless be derived from the EXAFS analysis on the nature of these species.

Acknowledgments

We kindly thank N. Haack and M. Hermann (station X1.1 at Hasylab, Hamburg) for the help provided during the X-ray absorption measurements. The European Union program for Large Scale Facilities (Contract No. ERBFMGECT950059) and NWO (Contract No. 326-710) are acknowledged for financial support.

References

[1] E.M. El-Malki, R.A. van Santen, W.M.H. Sachtler, J. Catal. 196 (2000) 212.
[2] H.-Y. Chen, W.M.H. Sachtler, Catal. Today 42 (1998) 73.
[3] H.-Y. Chen, T. Voskoboinikov, W.M.H. Sachtler, J. Catal. 180 (1998) 171.
[4] H.-Y. Chen, T. Voskoboinikov, W.M.H. Sachtler, Catal. Today 54 (1999) 483.
[5] H.-Y. Chen, X. Wang, W.M.H. Sachtler, Appl. Catal. A 194–195 (2000) 159.
[6] Z.-X. Gao, Q. Sun, W.M.H. Sachtler, Appl. Catal. B 33 (2001) 9.
[7] T. Voskoboinikov, H.-Y. Chen, W.M.H. Sachtler, J. Molec. Catal. A 155 (2000) 155.
[8] H.-Y. Chen, E.M. El-Malki, X. Wang, R.A. van Santen, W.M.H. Sachtler, J. Molec. Catal. A 162 (2000) 159.
[9] A.V. Kucherov, M. Shelef, J. Catal. 195 (2000) 112.
[10] P. Marturano, L. Drozdová, G.D. Pirngruber, A. Kogelbauer, R. Prins, Phys. Chem. Chem. Phys. 3 (2001) 5585.
[11] A.A. Battiston, J.H. Bitter, F.M.F. de Groot, A.R. Overweg, O. Stephan, J.A. van Bokhoven, P.J. Kooyman, C. van der Spek, G. Vankó, D.C. Koningsberger, J. Catal. 213 (2003) 251.
[12] P. Marturano, L. Drozdová, A. Kogelbauer, R. Prins, J. Catal. 192 (2000) 236.
[13] L.J. Lobree, I.-C. Hwang, J.A. Reimer, A.T. Bell, J. Catal. 186 (1999) 242.
[14] A.A. Battiston, J.H. Bitter, W.M. Heijboer, F.M.F. de Groot, D.C. Koningsberger, J. Catal., in press.
[15] T.V. Voskoboinikov, H.-Y. Chen, W.M.H. Sachtler, Appl. Catal. B 19 (1998) 279.
[16] M. Vaarkamp, B.L. Mojet, F.S. Modica, J.T. Miller, D.C. Koningsberger, J. Phys. Chem. 99 (1995) 16067.
[17] M. Wilke, F. Farges, P.-E. Petit, G.E. Brown Jr., F. Martin, Am. Miner. 86 (2001) 714.
[18] M. Vaarkamp, J.C. Linders, D.C. Koningsberger, Phys. B 209 (1995).
[19] M. Vaarkamp, I. Dring, R.J. Oldman, E.A. Stern, D.C. Koningsberger, Phys. Rev. B 50 (1994) 7872.
[20] D.C. Koningsberger, B.L. Mojet, G.E. van Dorssen, D.E. Ramaker, Top. Catal. 10 (2000) 143.
[21] J.W. Cook, D.E. Sayers, J. Appl. Phys. 52 (1981) 5024.
[22] A.L. Ankudinov, J.J. Rehr, Phys. Rev. B 56 (1997) R1712.
[23] J. Iball, C.H. Morgan, Acta Crystallogr. 23 (1967) 239.
[24] R.L. Blake, R.E. Hessevick, T. Zoltai, L.W. Finger, Am. Miner. 51 (1966) 123.
[25] D.C. Koningsberger, Jpn. J. Appl. Phys. 32 (1993) 877.
[26] G.G. Li, F. Bridges, C.H. Booth, Phys. Rev. B 52 (1995) 6332.
[27] C.M. Fu, M. Deeba, W.K. Hall, Ind. Eng. Chem. Prod. R&D 19 (1990) 299.
[28] G.D. Lei, B.J. Adelman, J. Sárkány, W.M.H. Sachtler, Appl. Catal. B 5 (1995) 245.
[29] G. Busca, V. Lorenzelli, J. Catal. 72 (1981) 303.
[30] M.D. Amiridis, F. Puglisi, J.A. Dumesic, W.S. Millman, J. Topsøe, J. Catal. 142 (1993) 572.
[31] L.J. Lobree, I.-C. Hwang, J.A. Reimer, A.T. Bell, Catal. Lett. 63 (1999) 233.
[32] K. Hadjiivanov, H. Knözinger, B. Tsynstsarski, L. Dimitrov, Catal. Lett. 62 (1999) 35.
[33] K. Hadjiivanov, J. Saussey, J.L. Freysz, J.C. Lavalley, Catal. Lett. 52 (1998) 103.
[34] K.-I. Segawa, Y. Chen, J.E. Kubsh, W.N. Delgass, J.A. Dumesic, W.K. Hall, J. Catal. 76 (1982) 112.